Journal of Earthquake Engineering

STRONG GROUND MOTIONS AND DAMAGE PATTERNS FROM THE 1999 DUZCE EARTHQUAKE IN TURKEY

ELLEN M. RATHJE
Department of Civil, Architectural, and Environmental Engineering, University of Texas at Austin
1 University Station C1792
Austin, Texas 78712 USA

JONATHAN P. STEWART
Department of Civil and Environmental Engineering, University of California at Los Angeles
Los Angeles, CA USA

M. BORA BATURAY
GeoSyntec Consultants
Chicago, IL USA

JONATHAN D. BRAY
Department of Civil and Environmental Engineering, University of California at Berkeley
Berkeley, CA USA

J.P. BARDET
Department of Civil and Environmental Engineering, University of Southern California
Los Angeles, CA USA

Received (received date)
Revised (revised date)
Accepted (accepted date)

The M_w 7.1 Duzce earthquake occurred on 12 November 1999 along the North Anatolian Fault in northwestern Turkey. This paper documents observations from a field reconnaissance team, addressing two principal aspects of this significant earthquake: the recorded ground motions and the distribution and severity of the earthquake effects on the built environment. In general, the recorded ground motions from this earthquake were smaller than predicted by ground motion predictive equations available at the time of the event. One anomalous recording is presented and potential causes for this irregular motion based on observations from field reconnaissance are discussed. The effects of rupture directivity on the near-fault recordings are assessed and the effects of soil conditions on the recorded ground motions are examined. The patterns of building damage based on post-earthquake reconnaissance are presented for the most strongly shaken cities in the near-fault region: Duzce, Kaynasli, and Bolu. Damage in Duzce was concentrated in the southern part of the city, which is underlain by softer sediments. Damage in Bolu was distributed evenly throughout the city; whereas damage was concentrated on more recent alluvial sediments in Kaynasli. No evidence of liquefaction or ground failure was observed in the populated areas surveyed after the earthquake.

Keywords: Duzce earthquake, strong ground motion, damage patterns.

1. Introduction

The M_w 7.1 Duzce earthquake occurred on 12 November 1999 along the North Anatolian Fault in northwestern Turkey. The Duzce earthquake was a right-lateral strike-slip event that ruptured a section of the North Anatolian Fault immediately to the east of the fault rupture from the 17 August 1999 Kocaeli (M_w 7.4) earthquake (Figure 1). This paper presents observations from a post-earthquake reconnaissance team supported by the United States National Science Foundation. Accordingly, two principal aspects of this significant earthquake are considered: an engineering evaluation of the recorded strong ground motions and an assessment of severity and distribution of the earthquake effects on the built environment based on field reconnaissance shortly after the earthquake.

Strong ground motions from the Duzce earthquake were recorded at 24 locations within 200 km of the fault. Because of the earthquake's relatively large magnitude, this strong motion dataset is important for future updates of ground motion predictive relationships. This paper presents the recordings from the Duzce earthquake and compares the recorded data with ground motion predictive equations available at the time of the event. The ground motions are critically evaluated and one anomalous recording is identified. The effects of near-fault rupture directivity and geologic conditions on ground motions are also assessed.

Results of field reconnaissance performed within two weeks of the event reveal the severity and distribution of earthquake effects on the built environment. The reconnaissance effort was focused on the largest population centers in the near-fault region: Duzce, Kaynasli, and Bolu. The distribution of geologic conditions in these areas is presented, along with damage data provided by municipalities and obtained from detailed field reconnaissance.

2. Strong Ground Motions

Twenty-four strong ground motions were recorded during the 1999 Duzce (M_w = 7.1) earthquake within 200 km of the fault. Ground motions were recorded by permanent recording stations operated by the Kandilli Observatory and Earthquake Research Institute (Kandilli) and the Earthquake Research Department of the General Directorate of Disaster Affairs (ERD) in Turkey. Additionally, temporary recording stations installed by the Lamont Doherty Earth Observatory of Columbia University (LD) recorded ground motions during the earthquake (Seeber 2000). These stations had been placed along the eastern end of fault rupture from the 17 August 1999 Kocaeli earthquake in an effort to collect aftershock data and fortuitously captured the Duzce earthquake mainshock. The locations of these stations, the fault rupture locations from the Kocaeli and Duzce earthquakes, and the regional geology are shown in Figure 1.

2.1. *Geologic conditions and site classes*

The geology in the affected region ranges from hard Mesozoic bedrock in mountain ranges to large sediment-filled, pull-apart basins formed by the North Anatolian fault system. The major alluvial basins affected by the earthquake were the Duzce and Bolu

basins (Figure 1). North and south of these basins, pre-Miocene basement rock conditions are found. The ERD typically operates a single strong motion station in each major town along the North Anatolian fault. Consequently, most of the permanent stations located close to the fault are ERD stations, and two of these stations are located within 20 km of the fault. Because most of the towns along the North Anatolian fault are located in large alluvial basins, most of the ERD stations are founded on deep alluvium. The LD stations were strategically placed close to the surface trace of the fault rupture from the Kocaeli earthquake (Figure 1). In this area, the fault runs along a mountain rangefront that separates the Adapazari and Duzce alluvial basins. As a result, the LD stations are located on stiffer materials than the near-fault ERD stations. However, many of these stations were situated on hillsides where topography may have affected the recorded ground motions. The permanent Kandilli stations are located in the Istanbul area, a significant distance from the fault (i.e., greater than 100 km). The geology in this region ranges from hard rock along the Bosphorus Strait to soft rock and deep soils west of Istanbul.

General site classifications were assigned to the stations based on regional geology (Figure 1), visits to strong motion stations, discussions with station owners, and results from shear wave velocity testing (Rosenblad et al. 2001, Rathje et al. 2003). These site classifications are indicated in Table 1 for each recording station. Geomatrix (1993) site classes, Simplified Geotechnical Site (SGS) classes (Rodriguez-Marek et al. 2001), and International Building Code (ICC 2003) site classes were assigned to each station and these classification systems are defined in Table 2. The Geomatrix and SGS classification systems are based only on a general description of the soil profile, distinguishing shallow soil and rock sites from deep soil and soft soil sites. The Geomatrix and SGS classes are indicated for each station because they can be initially defined using only limited information on regional and local geology. The International Building Code (IBC) classes are based on the average shear wave velocity over the top 30 m of the soil deposit ($\overline{V_s}$). Hence, the IBC classifications are only indicated for stations where results from shear wave velocity testing were available. The Spectral Analysis of Surface Waves (SASW) method (Stokoe et al. 1994) was used to measure shear wave velocities at thirteen strong motion stations affected by the Duzce earthquake (Rosenblad et al. 2001, Rathje et al. 2003).

The number of strong motion stations founded on rock/shallow soil (3 rock sites, 10 shallow stiff soil sites) is relatively similar to the number of stations on deep soil (10 sites). However, the majority of the deep soil stations are located more than 100 km from the fault (Table 1). The limited strong motion data at soil sites in the near-fault region limits the information that can be assessed from this earthquake regarding seismic site response in the near-fault region under strong shaking conditions.

The only soft site recording is at Ambarli (Table 1), with $\overline{V_s}$ ~ 170 m/s. The Duzce station is a borderline soft soil site with 3.1 m of surficial material with shear wave velocities below 180 m/s. However, this material cannot be definitively described as soft clay from solely the V_s measurements and $\overline{V_s}$ for the entire top 30 m is equal to 275 m/s.

2.2. *Comparison with ground motion prediction equations*

The recorded ground motions obtained from the various operating agencies were high pass filtered and baseline corrected. Peak ground accelerations (PGA, geometric mean of the horizontal components) and peak ground velocities (PGV, geometric mean of the horizontal components) are plotted versus closest distance in Figure 2. Also shown in Figure 2 are median predictions of PGA from the pre-1999 ground motion predictive relationships of Idriss (1995) and Abrahamson and Silva (1997), and PGV predictions from Campbell (1997); all relationships are for a strike-slip focal mechanism, rock site conditions, and M_w = 7.1. The data in Figure 2 are separated between rock/shallow soil sites (Geomatrix classes A and B, SGS classes B and C), deep soil sites (Geomatrix and SGS class D), and soft soil sites (Geomatrix and SGS class E). For PGA, the majority of the rock/shallow soil data fall close to or below the minus 2 standard deviation curve in Figure 2(a). Although less than 1 km from the fault, the LD-7 station recorded a PGA < 0.1 g.

The data in Figure 2 indicate that ground motions in the near-fault region are smaller than expected, which is similar to observations made from the Kocaeli earthquake data (Rathje et al. 2000, Durukal 2002). However, the Duzce earthquake ground motions recorded at rock/shallow soil sites were unexpectedly small up to distances as great as 100 to 200 km (Figure 2(a)); whereas the Kocaeli earthquake rock/shallow soil motions were unexpectedly small only at distances less than about 20 km (Rathje et al. 2000). The only rock/shallow soil motion from the Duzce earthquake that plots above the median prediction is LD-4. This station was situated on a moderately steep slope and upslope from a landslide that occurred during the earthquake; these conditions may have affected the recording. This motion will be discussed later in detail.

In the near-fault region (i.e., less than 20 km from the rupture), the only deep soil recording stations are Duzce (DZC, PGA ~ 0.45 g) and Bolu (BOL, PGA ~ 0.77 g). The PGA values at both of these sites are greater by factors of approximately 3 to 5 than those at rock/shallow soils sites recorded at similar distances (Figure 2(a)). The BOL and DZC stations have similar values of shear wave velocity ($\overline{V_s}$ = 290 m/s BOL and $\overline{V_s}$ = 275 m/s DZC), although a 0.6 m thick layer of 90 m/s shear wave velocity material is located near the surface at the BOL station. This soft layer is underlain by material with V_s = 200-250 m/s. Soil in an open field near the Bolu station was observed to be highly plastic (e.g., large shrinkage cracks), indicating that the surficial soils are cohesive. The BOL instrument is located in a 1-story building on a concrete block isolated from the building's slab foundation, which was not significantly damaged during the earthquake. However, the 1-story building is in close proximity to a significantly damaged 5-story building, which may have affected the recording.

In the far-field region (i.e., greater than 100 km from the rupture) most of the deep soil data fall below the median prediction for rock (Figure 2(a)). The largest motions in the far field were recorded at Ambarli (ATS) and Fatih (FAT) in Istanbul. PGA values at these stations (~0.03 g) were about four times as great as those recorded on neighboring rock/shallow soil (~0.008 g). Similar amplification occurred at ATS during the Kocaeli

earthquake (Rathje et al. 2000, 2003). SASW testing at ATS indicates that the shear wave velocity near the surface is less than 100 m/s and the shear wave velocity does not exceed 180 m/s in the top 25 m (Rosenblad et al. 2001). Accordingly, it appears that the soft soils at ATS locally amplified the ground shaking. The other far-field deep soil motions indicate amplification of PGA on the order of 3 with respect to the far-field rock motions.

The PGV data from rock and shallow soil sites (Figure 2(b)) are generally within the plus and minus 2 standard deviation predictions from Campbell (1997). The notable exceptions are at distances greater than 100 km, where the rock/shallow soil data are above the plus 2 standard deviation prediction. However, the Campbell (1997) PGV relationship was derived from data recorded at distances less than 50 km, and therefore, it may not be valid for larger distances. In the near-fault region, the PGV from the DZC and BOL records are noticeably larger than the plus 2 standard deviation prediction. These large values of PGV indicate enhanced moderate period energy and are most likely a result of deep soil response (DZC) and/or forward rupture directivity effects (BOL). At distances larger than 100 km, the deep and soft soil sites display significantly larger values of PGV than the rock/shallow soil sites because of the influence of soil conditions.

Pseudo-spectral accelerations for 5% damping at periods of 0.3 s and 1.0 s were calculated for the horizontal components of the ground motions, and their geometric means are plotted versus distance in Figure 3. Also shown are the Idriss (1993, 1995) and Abrahamson and Silva (1997) ground motion predictive relationships (rock site conditions, M_w = 7.1, strike-slip focal mechanism). As with PGA, the data for rock/shallow soil at T = 0.3 s (Figure 3(a)) are significantly smaller than the model predictions. The deep soil data are above the median rock prediction in the near-fault region, but are below the median rock prediction in the far field. At all distances deep soil motions at T = 0.3 s are larger than those on rock/shallow soil by factors ranging from 2 to 4. At T = 1.0 s (Figure 3(b)), the rock/shallow soil data remain below the median prediction. However, the deep soil data at all distance ranges fall above the median rock prediction and the difference relative to the rock/shallow soil sites is a factor of approximately 4 to 8. The significant increase in long period energy in the near-fault soil motions may be a result of one-dimensional site amplification, basin effects, or enhanced site amplification due to fault rupture directivity.

The frequency content and duration of the recorded ground motions are compared with pre-1999 predictive relationships in Figure 4. Frequency content is expressed by the mean period (T_m), which is calculated by averaging the Fourier amplitude coefficients over the frequency range of 0.25 to 20 Hz (Rathje et al. 1998). Significant duration ($D_{5\text{-}95}$) is expressed as the time between the build up of 5% and 95% of the Arias intensity (Arias 1969). Mean period is plotted versus distance and compared with the relationships proposed by Rathje et al. (1998) for rock/shallow soil sites in Figure 4(a). In general, the mean period of the recorded ground motions increases with distance and the data fall within plus and minus one standard deviation of the median prediction (Figure 4(a)). In the near-fault region, the LD-7 station at less than 1.0 km displays a large T_m, which may

be caused by its close proximity to the fault and the 20 to 40 cm of permanent displacement indicated in the displacement-time histories, referred to as fling-step (Stewart et al. 2002). Only a few stations in the far-field fall above the plus one standard deviation prediction, and these stations were situated on deep soil that would tend to enhance the long period energy in the ground motion.

Significant duration is plotted versus distance and compared with the relationship proposed by Abrahamson and Silva (1996) for rock/shallow soil sites in Figure 4(b). Almost all of the data lies within plus and minus one standard deviation of the median prediction. The duration of shaking at BOL is smaller than the other near-fault stations, most likely because of the effects of forward directivity. Somerville et al. (1997) predicts a reduction in duration of about 20% based on the location of the BOL station with respect to the epicenter of the earthquake.

2.3. *Discussion of Stations LD-4 and LD-8*

Eight ground motions were recorded within 20 km of the fault during the Duzce earthquake. Six of these recordings are from temporary stations installed by the Lamont Doherty Observatory at shallow soil sites (LD-4, LD-5, LD-7, LD-8, LD-10, LD-12) and two are from ERD stations situated on deep soil (DZC, BOL). The majority of the LD data fall significantly below the median prediction of motion for rock/shallow soil sites (Figures 2, 3), with the exception of the LD-4 station.

The LD-4 station is located 8.2 km from the fault and less than 0.5 km south of the LD-8 station. These stations are located on opposite sides of the same east/west trending valley. The acceleration, velocity, and displacement-time histories of the fault normal components (FN, 000 azimuth) recorded at LD-4 and LD-8 are shown in Figure 5. The LD-4 station recorded a PGA of 0.89 g in the FN direction, while LD-8 recorded 0.15 g. When the acceleration-time histories are integrated to velocity-time histories the waveforms look similar, and the displacement-time histories are almost identical. Additionally, the spectral acceleration at 1.0 s for LD-4 is similar to the other near-fault motions (Figure 3(b)), while the PGA and spectral acceleration at 0.3 s are much larger for LD-4 (Figures 2(a), 3(a)). These observations indicate that the long period energy in the two records is similar, but there is a significant difference in the high frequency components of motion.

Examining the Fourier amplitude spectra of the two motions indicates that the LD-4 motion has significantly more high frequency energy; with the LD-4 Fourier amplitudes 5 to 10 times larger than the LD-8 Fourier amplitudes at frequencies greater than 2 Hz. Possible explanations for the enhanced high frequency energy recorded at LD-4 include vibrations associated with a nearby landslide, local site amplification, and topographic amplification. The LD-4 station was founded on a moderately steep hillside that experienced a landslide during the Duzce earthquake (Figure 6). The instrument was located upslope from the landslide, as shown in Figure 6. The downslope movement of the soil in the landslide may have affected the recording at LD-4. However, if the landslide was the main reason for the larger ground motions at LD-4, the motions from

LD-4 and LD-8 should appear similar during the initial part of the record, assuming that it took some time for the slide to initiate. The acceleration-time histories in Figure 5 from LD-4 and LD-8 do not have similar amplitudes in the beginning of the record, suggesting that the slide initiated immediately after strong shaking began or that the slide did not have a significant effect on the LD-4 recording. Nonetheless, the occurrence of a shallow slide near the LD-4 instrument indicates that there is a surficial layer of softer, residual soils. These softer soils may have amplified the high frequency motion at the site. Finally, the presence of the slope itself may have induced some topographic amplification. Unfortunately, the area surrounding LD-4 and LD-8 is sparsely populated (see Figure 6), and thus it is not possible to compare damage patterns near the two stations. However, note that the reinforced-concrete structure in the foreground of Figure 6 was not damaged, although it was very close to the LD-4 station.

2.4. *Evaluation of Near-Fault Rupture Directivity*

Near-fault ground motions within 20 km of the fault can display rupture directivity effects. Forward-directivity occurs when the rupture propagates towards a site and the site is aligned with the direction of slip (Somerville et al. 1997). Forward-directivity motions display enhanced long period energy, and the fault normal component of long period motion is greater than the fault parallel component. For strike-slip events, forward rupture directivity is expected near the ends of the fault rupture, away from the epicenter. Based on the location of the near-fault stations (Figure 1), the location of the earthquake epicenter, and the bilateral rupture of the earthquake, the BOL and LD stations are expected to display forward rupture directivity characteristics. The DZC station is located directly north of the epicenter of the earthquake, and according to the work of Somerville et al. (1997) it should not display the effects of forward-directivity.

The ratio of fault normal to fault parallel (FN/FP) spectral acceleration is plotted versus period in Figure 7 for the near-fault stations that are less than 20 km from the fault. Motions displaying significant forward -directivity characteristics will have FN/FP ratios considerably greater than 1.0 in the long period range. The motion that displays the largest FN/FP ratios is BOL (Figure 7(a)), with values in excess of 1.5 at periods greater than about 2.5 s. For comparison, the FN/FP ratios for DZC are close to or less than 1.0 at longer periods. Most of the LD records, which were recorded off the western edge of the fault (Figure 1), do not display any systematically large FN/FP ratios at long periods (Figures 7(a), (b)). The LD-8 motion does show some rupture directivity in the period range of 2.0 to 5.0 s. Somerville (2003) proposed relationships for the period of the forward-directivity velocity pulse as a function of magnitude. This model predicts a pulse period of approximately 2.0 s for a M_w 7.1 earthquake, and this pulse would be expected to cause a peak in the FN/FP ratio close to this period. However, the large FN/FP ratios in Figure 7(a) occur at periods larger than 2.0 s.

The LD-7 station, located less than 1.0 km from the western terminus of the fault rupture, does not show significant forward-directivity characteristics. The LD stations

located further from the fault (i.e., LD-5, LD-10, LD-12) also do not show significant FN/FP ratios (Figure 7(b)). The absence of significant forward-directivity characteristics in the motions off the western edge of the fault may be a result of the slip distribution along the fault rupture. The slip inversion of Bouin et al. (2004) indicates that slip along the fault east of the hypocenter was on the order of 2 to 5 m, while the portion of the fault west of the hypocenter generally experienced less than 2 m of slip. The larger slip would be expected to cause rupture directivity effects to be more pronounced off the eastern terminus of the fault rupture (i.e., towards Bolu).

To further examine directivity effects, the displacement response spectra for the fault normal and fault parallel components of motion recorded at BOL, LD-8, and LD-7 (the stations closest to the edges of the fault rupture) are shown in Figure 8. The displacement spectrum for BOL (Figure 8(a)) shows classic forward rupture directivity characteristics, with the fault normal component significantly larger than the fault parallel component at long periods. The spectra start to deviate at periods greater than 2 s, and the spectral displacement in the fault normal direction is more than twice that in the fault parallel direction at a period of 5 s. Differences between the fault normal and fault parallel displacement spectra in the LD-8 record are also observed (Figure 8(b)), although the difference is less pronounced. Here, the spectral displacement in the fault normal direction is larger than that in the fault parallel direction at periods between about 2 and 4.5 s. However, the spectral displacements for the two components become similar again at a period of 5 s. No forward-directivity effects are observed in the LD-7 motion (Figure 8(c)), as the spectral displacements in the fault parallel and fault normal directions are similar at all periods.

2.5. *Evaluation of Site Effects from Nearby Recordings at Rock and Soil Sites*

Several strong-motion recording stations were located in Istanbul and allow for a comparison of ground shaking across different site classes. In Istanbul, one station was situated on rock/shallow soil (IST), four stations were founded on deep soil (CNA, DHM, FAT, KMP), and one station was situated on soft soil (ATS). No shear wave velocity information is available for the deep soil sites DHM, FAT, and KMP; therefore, the site classifications for these stations are considered best estimates.

The acceleration response spectra (geometric mean of the two horizontal components) from recordings made in Istanbul are shown in Figure 9(a) for rock/shallow soil (1 site), deep soil (4 sites), and soft soil (1 site) sites. The rock/shallow soil spectrum is significantly smaller than the others, particularly at periods less than 1.0 s. The deep soil sites amplified the PGA and maximum spectral accelerations. The deep soil site at FAT has notably large spectral accelerations in the T ~ 0. 5 s range, while the DHM deep soil site displays notably large spectral accelerations between T = 1.0 and 2.0 s. Generally, the soft soil site amplified the rock motion more than the deep soil sites, particularly at periods greater than 1.0 s.

Response spectral ratios, defined as the spectral acceleration on soil divided by the spectral acceleration on rock/shallow soil, are given in Figure 9(b). The reference (rock)

site and soil site motions have similar source and path contributions, and hence the spectral ratios shown in Figure 9(b) can be used to infer the local site amplification (per the reference site approach described by Field and Jacob 1995). The deep soil sites amplified the rock motion by about a factor of 3 at low to moderate periods (T < 0.5 s). This amplification increases to about 5.0 at periods around 1.0 s, but quickly drops below 1.5 at periods greater than 2.0 s. The observed amplification factors are significantly larger than those estimated using current semi-empirical and empirical models. For example, the International Building Code (ICC 2003) uses a short period amplification factor of 1.6 and a long period amplification factor of 2.4 for D (deep stiff soil) sites shaken by low intensity rock motions. Pre-1999 ground motion prediction equations (e.g., Abrahamson and Silva 1997, Boore et al. 1997) generally use short period amplification factors around 1.2 and longer period amplification factors between 1.5 and 2.0 for the low levels of reference site motions present in Istanbul during this earthquake.

Figure 9(b) also shows the uncertainty in the median amplification factors for the deep soil sites. With only four deep soil motions, the inherent variability in the amplification factors cannot be accurately assessed, but the uncertainty in the amplification factors computed from the limited data set can be evaluated. The standard deviation of the median amplification factor ($\sigma_{ln,median}$) at each period was computed as the standard deviation of the natural logarithm of the amplification factors divided by the square root of the number of observations ($\sigma_{ln,median} = \sigma_{ln} / \sqrt{n}$, with $n = 4$ for this case, Field and Jacob 1995). Over most periods, $\sigma_{ln,median}$ is between 0.15 and 0.2, but is increases to values between 0.35 and 0.4 at $T \sim 0.5$-0.6 s and $T \sim 1.5$-3.0 s. These period ranges represent the periods in which the spectral accelerations at FAT and DHM, respectively, are significantly different than the other deep soil sites (Figure 9(a)).

The soft soil site (ATS) shows considerable amplification of PGA and spectral accelerations at periods greater than 0.5 s (Figures 9(b)). The amplification at T < 0.1 s is about 4.5, and this amplification reduces to about 3 at T = 0.3 s. This "valley" of amplification is often observed in one dimensional analytical seismic site response predictions for soft soil sites because soil damping attenuates high frequency motions. In fact, in this period range the observed soft soil amplification is statistically indistinguishable from the deep soil amplification (Figure 9(b)). At periods between 1.0 and 5.0 s, the observed soft soil spectral amplification ranges from 8.5 to 4.0 with an average of about 5.5. Again, these observed amplification factors are larger than those incorporated in the International Building Code (ICC 2003) for E sites (Amp = 2.5 at short periods, = 3.5 at long periods). The large spectral accelerations at long periods at ATS are most likely a result of the soft soils at the site, although the site is also situated within a relatively narrow alluvial basin and may have experienced basin effects. It is interesting to note that the large spectral accelerations at long periods recorded at the DHM deep soil site are almost as large as the ATS spectral accelerations at periods between 1.5 and 3.0 s (Figure 9(a)). These large spectral accelerations may indicate that softer soils underlie the DHM station or that the soils at DHM are deep and the natural period of the site is long.

3. Damage Patterns

During the field reconnaissance, field surveys of damage were performed in Duzce, Kaynasli, and Bolu. These areas represent the major cities and towns in the near-fault region. Geologic data and additional damage data were compiled from studies performed after the earthquake by the various municipalities.

3.1. *Duzce*

The City of Duzce is located near the epicenter of the Duzce earthquake (Figure 1), approximately 7 km north of the fault rupture surface. As shown in Figure 2, the DZC strong motion station, which is located on Quaternary sediments, recorded a geometric mean peak acceleration of 0.43 g. A large number of buildings in Duzce suffered damage and/or collapse, resulting in 478 reported fatalities as compared to 264 during the Kocaeli earthquake (Basbakanlik 2000). The population of Duzce at the time of the earthquake was approximately 76,038 (DIE 1997).

The word “Duzce” in Turkish translates as “planar,” and the city was so-named due to its location on a plateau with 0.5-3º inclination to the southwest. The city is underlain entirely by Quaternary alluvial flood plain sediments (MREI 2000a). Surficial geotechnical conditions in these sediments have been investigated as part of a study commissioned by the Duzce municipal government (Bayindirlik 2000). Borings were drilled at 185 locations to depths of 10 to 20 m, and shear wave and compression velocities were evaluated at another 115 locations using the seismic refraction method. Although refraction is not the ideal method for measuring wave velocities for earthquake ground motion predictions, refraction velocities were the only data available from the municipality and they still represent useful information for comparative purposes. Soil conditions were found to consist principally of silts and clays, with interbeds of sands and gravels (Bayindirlik 2000). The thickness of these sediments is reported to be approximately 175 to 225 m. Relatively low shear wave velocities were found in the districts Aziziye, Uzunmustafa, Kultur, Kiremitocagi and Camikebir (located between the D-100 highway and the Asar river, Figure 10). Larger shear wave velocities were found in districts north of the D-100 highway, although the soil composition is similar. It is noted that the DZC strong motion station is located on the relatively soft materials south of the D-100 highway (Figure 10), an observation later confirmed by Rathje et al. (2003) who found $\overline{V_s}$ = 275 m/s and values as low as 150 m/s in the top 5 m.

The Bayindirlik (2000) study also outlined zones considered to have high liquefaction potential, and these zones are shown in Figure 10. The liquefaction potential was evaluated by a SPT-based method; however, the specific procedures by which these zones were defined are poorly documented. No evidence of liquefaction was found during detailed field surveys inside and outside of these zones, even though a river with a 3 m-high bank cuts through the heart of the city. As this area was strongly shaken, this implies a low liquefaction potential in the region. Additionally, it was noted during field reconnaissance that many buildings had basements and that several open excavations were not filled with water, which indicates that the ground water table must be at least 3-

m deep. The location of the ground water table may have played a role in the absence of liquefaction during this earthquake. The Bayindirlik (2000) study indicates that the lowest groundwater levels occur during the month of October. Although no liquefaction was observed, the zones in Figure 10 may still indicate locations of relatively recent and poorly consolidated sediments. Ground settlements of 1 to 2 cm were observed adjacent to buildings at a few isolated locations in Duzce (Figure 11).

The building stock in Duzce consists principally of 4 to 5 story reinforced concrete structures in the downtown area (Uzunmustafa, Kultur, Camikebir, Serefiye, Burhaniye, Nusrettin, Cedidiye), with 2 to 3 story buildings of timber construction with brick in-fill walls being more common in outlying areas. The Duzce municipal government documented damage to the building stock, and based on these data the percentages of heavily damaged and collapsed buildings were compiled by district (Table 3 and Figure 10). The damage distribution in Figure 10 shows higher damage rates south of the D-100 highway, which is consistent with the lower shear wave velocities reported in these areas (Bayindirlik 2000).

Many of the buildings reflected in these statistics were originally damaged during the August 1999 Kocaeli earthquake. These buildings typically had been marked with an 'X' after the Kocaeli event to indicate they were unsafe to occupy (e.g., Figure 12). It is not known what percentage of the buildings reported as damaged following the Duzce event had originally been damaged by the Kocaeli event, although visual observations of the 'X' markings by the authors suggest this ratio to be less than one third.

Detailed building-by-building surveys of structural and foundation damage were performed along two crossing "lines" passing through the downtown areas (locations in Figure 11). No significant ground deformations were observed in any of the inspected buildings, so the data reported here are limited to structural performance, which is quantified using the damage index system listed in Table 4. The north-south line started from the D-100 freeway and extended 2.3 km south through downtown and to the limit of significant development. The 2.8 km east-west line also passes through the downtown area, and development at either end is relatively sparse.

As indicated in Figure 13, the first 0.4 km of the EW line has principally 2 to 5 story buildings with variable damage levels. Damage is substantial from 0.4 to 1.0 km, with most structures having collapsed. Many of these structures had been previously damaged during the Kocaeli earthquake (e.g., Figure 12(a)). Buildings along the remainder of the line (1.0 to 2.8 km) generally are only moderately damaged (D1-D2). These results are generally consistent with the district damage rates shown in Figure 11. Buildings along the NS line showed generally light damage north of the Asar river (0 to 1.1 km), but zones of relatively concentrated damage south of the river. This concentration of damage south of the river is not reflected in the district damage rates in Figure 11. The absence of damage to basement walls and retaining walls due to seismic earth pressures was also noted. The damage patterns in Figures 13 do not indicate any clear association of damage with the mapped liquefaction zones by Bayindirlik (2000). Figure 14 shows that relatively tall buildings (>4 stories) suffered the highest damage rates. It is unknown to

what extent this trend of increasing damage with story height is associated with variability in construction standards and/or preferential sediment amplification of intermediate to long period ground motions. However, the recorded ground motions from the DZC station indicate large spectral accelerations in the T = 0.4 to 0.8 s range, which tends to match the period range of these taller structures.

In Duzce and other areas affected by the Kocaeli earthquake, retrofit measures had been undertaken to provide confinement for reinforced concrete columns in frame buildings. One such building is shown in Figure 15, with a detail view of the column confinement system indicated in the inlay. These retrofitted buildings appeared to perform well. The building in Figure 15 provides a clear indication of the retrofit effectiveness. Most of the perimeter columns in this structure had been retrofitted, with the exception of some of the second story columns. The collapse was caused by the failure of the second story corner column nearest the photographer in Figure 15.

3.2. *Kaynasli*

Kaynasli is located along the eastern margin of the Duzce fault valley, between the Asar River to the north and the foot of the Guney Mountains to the south. Concentrated structural damage in portions of Kaynasli resulted in 313 fatalities (Kaynasli 2000) out of a population of 10,132. No ground motion recordings are available in Kaynasli. The fault rupture passes along the northern margin of the town (Figure 16) and beneath many structures. However, here we focus on damage that occurred in areas away from the fault rupture and do not consider the effect of the surface fault rupture on structures

As shown in Figure 16, the surface geology in Kaynasli consists of Eocene flysch in the hills south of town and Quaternary alluvial sediments to the north. The “downtown” area is located in a small alluvial valley cut into the hillside (Figure 16). The Kaynasli municipal government commissioned a geotechnical study in which 79 borings of 10 m depth were drilled across the town. Seismic wave velocities were also measured with refraction techniques. From these data, the alluvial sediments were found to consist generally of interbedded silty sands and sandy clays. Flysch deposits are significantly weathered to at least 10 m depth. Seismic compression wave velocities in the alluvial and flysch deposits are on the order of V_p = 100-300 and 400-500 m/s, respectively.

The building stock in Kaynasli consists of 3 to 5 story reinforced concrete frame structures and 1 to 3 story timber/brick structures. Reinforced concrete structures are most common in the downtown area (Merkez district), while timber/brick construction is more common in surrounding areas. Some of the reinforced concrete structures were of unusually poor quality, with no reinforcement connecting structural members (e.g., Figure 17).

The Kaynasli municipal government compiled information on the damage to each structure in the town, and this information is shown in Figure 16 and summarized in Table 5. The damage classifications used in Figure 16 and Table 5 were developed by local engineers. Delineations between damage levels are generally poorly defined, although the distinction between heavy and medium damage is made on the basis of

whether buildings can be safely occupied. Nonetheless, the data provide a good qualitative picture of damage patterns that is consistent with rapid visual surveys of the area by the authors.

Buildings in the downtown area (Merkez District) suffered a collapse rate of 64%, whereas buildings further to the west (and somewhat closer to the fault) had collapse rates on the order of 25 to 30%. Figures 18 (a) and (b) show overviews of the downtown Merkez area and the less damaged Sariyer area further west. As shown on Figure 16, the downtown area is underlain by a southward protrusion of the alluvium along the flysch/alluvial boundary. Less damaged areas further to the west are underlain by flysch deposits. This apparent association of damage with surface geology suggests possible ground motion amplification in the shallow alluvial sediments.

As noted previously, visual inspections of the Kaynasli region revealed damage patterns consistent with those from the municipal data. Foundation inspections for 185 buildings throughout the region revealed no evidence of settlement or ground deformations (except in areas affected by fault rupture). No sand boils were observed. Accordingly, there is no evidence that liquefaction occurred in Kaynasli, despite the shallow groundwater depth of 1 to 4 m within the alluvial soils (Kaynasli 2000).

3.3. *Bolu*

The City of Bolu is located half way between Ankara and Istanbul, approximately 15 km east of the eastern terminus of the fault rupture. As shown in Figure 2, the BOL strong motion station, which is located on Quaternary alluvium, recorded a geometric mean peak horizontal acceleration of 0.75 g. Many buildings were damaged significantly during the Duzce earthquake, but few collapsed and thus the death toll (48) was minimal relative to Duzce and Kaynasli. The population of the city at the time of the earthquake was about 80,225 (DIE 1997).

As shown in Figure 19, Bolu is primarily underlain by Quaternary alluvium (MREI 2000b). Early development in Bolu occurred on the outcropping Pliocene bedrock in the center of town (Figure 19), with more recent development (in the past three decades) occurring on the surrounding Quaternary alluvium. Following the Duzce earthquake, the Bolu municipal government funded the drilling of 223 borings of 6 to 25 m depth, along with the measurement of shear wave velocity at 22 locations. Unfortunately, this information has not yet been made publicly available.

The buildings in Bolu consist primarily of 2 to 3 story timber construction with brick infill walls as well as more recently constructed 4 to 5 story reinforced concrete structures. The Bolu municipal government surveyed the building stock after the Duzce earthquake and identified collapsed or heavily damaged structures (Bolu 2000), the locations of which are shown in Figure 19 (Baturay 2000). The inventory of damaged buildings in Figure 19 indicates no clear concentrations of damage, which may indicate that the soil conditions in the Quaternary alluvium are relatively uniform throughout the city. However, on Pliocene bedrock 4 to 5 story reinforced concrete structures had a

noteworthy lack of damage (i.e., damage in bedrock areas was primarily in short timber/brick construction). No evidence of liquefaction was observed in Bolu during rapid visual inspections of the area.

4. Conclusions

The 1999 Duzce earthquake was a significant earthquake that occurred directly east of the 1999 Kocaeli earthquake. This paper presents observations from the ground motions recorded during the earthquake and documents the effect of the earthquake on the built environment based on post-earthquake reconnaissance.

The strong ground motions recorded by permanent and temporary recording stations during the 1999 Duzce earthquake represent an important dataset for expanding our knowledge regarding strong ground motion during large earthquakes. The ground motions from the Duzce earthquake were lower in intensity than predicted by ground motion predictive relationships available at the time of the earthquake. The motions from the LD-4 temporary station are much larger than another temporary recording station nearby. The frequency content, as characterized by a scalar frequency content parameter, and the duration of the recorded motions from the Duzce earthquake were similar to predictions from pre-1999 predictive relationships. A comparison of ground motions recorded on rock and soil sites indicates amplification of motion, both in the near-fault and far-field regions. The observed amplification in the far-field region was significantly larger than those incorporated in the International Building Code and ground motion prediction equations. Rupture directivity effects were observed off the eastern edge of the fault where the fault slip was concentrated. Significant forward-directivity effects were not observed at the western end of the fault where the fault slip was relatively modest.

Field reconnaissance was performed by the authors after the earthquake in the main cities and towns in the near-fault region (Duzce, Kaynasli, and Bolu) and damage data for these areas were collected by the local municipalities. In Duzce and Kaynasli, severe damage was concentrated in areas underlain by softer and/or younger sediments. Damage was more relatively modest in the city of Bolu, but the damage that did occur was relatively evenly distributed in alluvial areas and absent in bedrock areas. No evidence of liquefaction or ground failure was observed in any of these cities.

Acknowledgments

The authors gratefully acknowledge the financial support provided by the National Science Foundation for the Duzce earthquake reconnaissance (CMS-0083058) and for shear wave velocity profiling at strong motion stations in Turkey (CMS-0085300). Comments from Drs. David Boore and Norman Abrahamson regarding the ground motion sections of this paper were particularly helpful. Special thanks to Jeff Bachhuber and the staff of William Lettis and Associates for drafting the map in Figure 1, and to Ms. Gulsel Baturay of Ankara, Turkey for collecting damage information from the affected municipalities.

References

Abrahamson, N.A. and Silva, W.J. [1996] Empirical Ground Motion Models. Report prepared for the Brookhaven National Laboratory, Brookhaven, NY.

Abrahamson, N.A. and Silva, W.J. [1997] "Empirical Response Spectral Attenuation Relations for Shallow Crustal Earthquakes," *Seismological Research Letters* 68(1), 94-127.

Arias, A. [1969] "A Measure of Earthquake Intensity," *Seismic Design for Nuclear Power Plants*. MIT Press.

Basbakanlik [2000] T.C. Basbakanlik Kriz Yonetim Merkezi (Turkish Crisis Management Center), http://www.basbakanlik.gov.tr/krizyonetimmerkezi/02subat2000basinbildirisi.htm (in Turkish).

Baturay, G. [2000] Personal Communication.

Bayindirlik [2000] T.C. Bayindirlik ve Iskan Bakanligi Afet Isleri Genel Mudurlugu, "Duzce Kenti - 1. Nolu Kesim 12 Kasim Depremi Sonrasi Yeniden Yapilanma Kapsaminda Jeolojik-Jeoteknik Inceleme Raporu" (Duzce City – Section 1 – Geologic and Geotechnical Investigation Report for Reconstruction after the 12 November Earthquake, in Turkish).

Bolu [2000] Bayindirlik ve Iskan Bakanligi Bolu Il Mudurlugu (in Turkish)

Boore, D., Joyner, W., and Fumal, T. [1997] "Equations for Estimating Horizontal Response Spectra and Peak Acceleration from Western North American Earthquakes: A Summary of Recent Work." *Seismological Research Letters* 68(1), 128-153.

Bouin, M.-P., Bouchon, M., Karabulut, H. and Aktar, M. [2004] "Rupture process of the 1999 November 12 Düzce (Turkey) earthquake deduced from strong motion and Global Positioning System measurements." *Geophysical Journal International*, 159(1), 207-211.

Bray, J.D. and Stewart, J.P. [2000] "Damage Patterns and Foundation Performance in Adapazari." in *Earthquake Spectra, The 1999 Kocaeli, Turkey, Earthquake Reconnaissance Report*, Earthquake Engineering Research Institute, 16(A), 163-189.

Campbell, K. [1997] Empirical Near-Source Attenuation Relationships for Horizontal and Vertical Components of Peak Ground Acceleration, Peak Ground Velocity, and Pseudo-Absolute Acceleration Response Spectra." *Seismological Research Letters*, 68(1), 154-180.

Coburn, A., and Spence, R. [1992] *Earthquake Protection.* West Sussex, England, John Wiley & Sons.

Devlet Istatistik Enstitusu, DIE [1997] 1997 Genel Nufus Tespitine Gore Il ve Ilcelerin Sehir ve Koy Nufuslari, http://www.die.gov.tr/istatistikler.htm (Populations of Cities and Towns and Villages according to the Results of 1997 Census, in Turkish).

Durukal, E. [2002] "Critical evaluation of strong motion in Kocaeli and Duzce (Turkey) earthquakes," *Soil Dynamics and Earthquake Engineering*, 22(7), 589-609.

Field, E.H. and Jacob, K.H. [1995] "A Comparison and Test of Various Site-Response Estimation Techniques, Including Three That Are Not Reference-Site Dependent," *Bulletin of the Seismological Society of America*, 85(4), 1127-1143.

Geomatrix Consultants [1993] Compilation of Geotechnical Data for Strong-Motion Stations in the Western United States. Report to Lawrence Livermore National Laboratory, Project No. 2256.

Idriss, I.M. [1995] "An Overview of Earthquake Ground Motions Pertinent to Seismic Zonation," *Fifth International Conference on Seismic Zonation*, Nice, France.

International Code Council. [2003] *International Building Code.*

Kaynasli, Yucel Musavirlik Muhendislik. [2000]. Duzce Ili Kaynasli Ilcesi Jeoteknik Zemin Etut Raporu (in Turkish).

Mineral Research and Exploration Institute, MREI [2000a]. Geologic map of Adapazari-G26-a3 region, Turkey, 1:25,000 scale.

Mineral Research and Exploration Institute, MREI [2000b]. Geologic map of Bolu-G27-d1 region, Turkey, 1:25,000 scale.

Rathje, E.M., Abrahamson, N.A., and Bray, J.D. [1998] "Simplified Frequency Content Estimates of Earthquake Ground Motions," *Journal of Geotechnical and Geoenvironmental Engineering.* ASCE, 124(2), 150-159.

Rathje, E.M., Stokoe, K.H., and Rosenblad, B.L. [2003] "Strong Motion Station Characterization and Site Effects during the 1999 Earthquakes in Turkey," *Earthquake Spectra*, Earthquake Engineering Research Institute, 19(3), 653-676.

Rathje, E. Idriss, I.M., and Somerville, P., [2000] "Strong Ground Motions and Site Effects," in *Earthquake Spectra, The 1999 Kocaeli, Turkey, Earthquake Reconnaissance Report*, Earthquake Engineering Research Institute, 16(A), 65-96.

Rodriguez-Marek, A., Bray, J. D., and Abrahamson, N. A. [2001] "An Empirical Geotechnical Seismic Site Response Procedure," *Earthquake Spectra*, The Professional Journal of the Earthquake Engineering Research Institute, (17) 1, 65-87.

Rosenblad, B., Stokoe, K.H., Rathje, E.M., and Darendeli, M. [2001] Characterization of Strong Motion Stations Shaken by the Kocaeli and Duzce Earthquakes in Turkey. Geotechnical Engineering Report GR01-1, Geotechnical Engineering Center, University of Texas, (also available at http://www.ce.utexas.edu/prof/rathje/research/turkey_velocity.html.)

Seeber, L. [2000] Personal Communication.

Somerville, P.G., Smith, N.F., Graves, R.W., and Abrahamson, N.A. [1997] "Modification of Empirical Strong Ground Motion Attenuation Relations to Include the Amplitude and Duration Effects of Rupture Directivity," *Seismological Research Letters*, 68(1), 199-222.

Somerville, P.G. [2003]. "Magnitude scaling of the near-fault rupture directivity pulse," *Physics of the Earth and Planetary Interiors*, 137, 201-212.

Stewart, J.P., Chiou, S.-J., Bray, J.D., Graves, R.W., Somerville, P.G., and Abrahamson, N.A. [2002]. "Ground motion evaluation procedures for performance based design," *Soil Dynamics and Earthquake Engineering*, 22 (9-12), 765-772.

Stokoe, K.H., Wright, S.G., Bay, J.A., and Roesset, J.M. [1994] "Characterization of Geotechnical Sites by SASW Method," in *Geophysical Characteristics of Sites*, Technical Committee 10 for XIII International Conference on Soil Mechanics and Foundation Engineering.

Table 1. Distances and site classifications for strong motion stations that recorded the Duzce earthquake

Station	Owner	Closest Distance (km)	Geomatrix Site Class[1]	SGS Site Class[1]	IBC Site Class[1]
Arcelik (ARC)	Kandilli	131.5	B	C	S_C
Ambarli (ATS)	Kandilli	188.7	E	E	S_E
Bursa Sivil (BRS)	ERD	167.3	A	B	--
Bolu (BOL)	ERD	12.0	D	D	S_D
Bursa Tofas (BUR)	Kandilli	166.1	D	D	--
Cekmece (CNA)	Kandilli	183.6	D	C	S_D
Aslan Cimento (DAR)	Kandilli	130.8	D	D	--
Hava Alani (DHM)	Kandilli	178.0	D	D	--
Duzce (DZC)	ERD	6.6	D	D	S_D
Fatih (FAT)	Kandilli	168.2	D	D	--
Istanbul (IST)	ERD	168.1	B	C	--
K.M. Pasa (KMP)	Kandilli	169.3	D	D	--
Kutahya (KUT)	ERD	168.3	D	D	--
Mudurnu (MDR)	ERD	34.3	A	B	--
Sakarya (SKR)	ERD	45.2	B	C	S_C
Yarimca (YPT)	Kandilli	97.5	D	D	S_D
LD-362 (LD-3)	LD	23.4	B	C	S_C
LD-375 (LD-4)	LD	3.9	B	C	--
LD-531 (LD-5)	LD	8.0	A	B	S_C
LD-1058 (LD-7)	LD	0.9	B	C	--
LD-1059 (LD-8)	LD	4.2	B	C	--
LD-1060 (LD-9)	LD	25.9	B	C	S_C / S_B
LD-1061 (LD-10)	LD	11.5	B	C	S_C
LD-1062 (LD-12)	LD	9.2	B	C	S_D

[1] Site classes derived from site visits, shear wave velocity measurements by Rathje et al. (2003), where available, local geology, and discussions with site owners.

Table 2. Site classification systems

Site Classes	**Soil Profile Description**	**Average $\overline{V}_s$ (m/s)**
Geomatrix (1993) Site Classification System		
A	Rock	--
B	Shallow Soil (soil depth < 20 m)	--
C	Deep Soil in Narrow Canyon (depth > 20 m, canyon < 2 km wide)	--
D	Deep Soil in Wide Canyon (depth > 20 m, canyon > 2 km wide)	--
E	Soft Soil V_s < 150 m/s	--
Simplified Geotechnical Site (SGS) Classification System Rodriguez-Marek et al. (2001)		
A	Hard Rock ($V_s \geq$ 1500 m/s)	--
B	Rock ($V_s \geq$ 760 m/s or < 6 m soil)	--
C	Weathered Rock, Shallow Stiff Soil (Soil depth < 60 m)	--
D	Deep Stiff Soil (Soil depth > 60 m)	--
E	Soft Soil (Soft clay thickness > 3 m)	--
IBC (2003) Site Classification System		
S_A	Hard Rock	> 1500
S_B	Rock	760 – 1500
S_C	Very Dense Soil and Soft Rock	360 – 760
S_D	Stiff Soil Profile	180 – 360
S_E	Soft Soil Profile	< 180

Table 3. Damage Statistics Collected by Duzce Municipality
(Bayindirlik 2000)

Districts	Medium Dmg. %	Heavy Dmg./Collapse %	#Collapses
Beyciler	0.8	0.4	2
Karaca	5	2.6	44
Hamidiye	0.4	4.6	76
Karahacimusa	0.3	0.1	2
Fatih	0.9	0.2	12
Yenimahalle	1.7	0.6	16
Aziziye	5.1	7.2	55
Uzunmustafa	4.1	4.7	95
Kultur	14.8	27.6	267
Serefiye	10.2	6.5	80
Burhaniye	12.9	5.4	76
Nusrettin	8.2	9.2	54
Cumhuriyet	0.6	0.6	6
Fevzi Cakmak	1.2	1.3	16
Cedidiye	3.8	0.9	67
Azmimilli	9.2	8.5	82
Cay	6.2	6.8	81
Camikebir	11.1	10.5	108
Kiremitocagi	3	2.4	31

Table 4. Structural Damage Index
(Bray and Stewart 2000, modified from Coburn and Spence 1992)

Index	Description	Interpretation
D0	No Observable Damage	No cracking, broken glass, etc.
D1	Light Damage	Cosmetic cracking, no observable distress to load bearing structural elements
D2	Moderate Damage	Cracking in load bearing elements, but no significant displacements across these cracks
D3	Heavy Damage	Cracking in load bearing elements with significant deformations across the cracks
D4	Partial Collapse	Collapse of a portion of the building in plan view (i.e. a corner, or a wing of building)
D5	Collapse	Collapse of the complete structure or loss of a floor of the structure.

Table 5. Damage statistics for districts in Kaynasli
(from Kaynasli 2000)

District	Heavy Dmg/Collapse %	Total # Bldgs.
Kumluca	40	206
Merkez	64	391
Sariyer	16	197
Karacali	17	271
Cele	59	17
Simsir	27	141

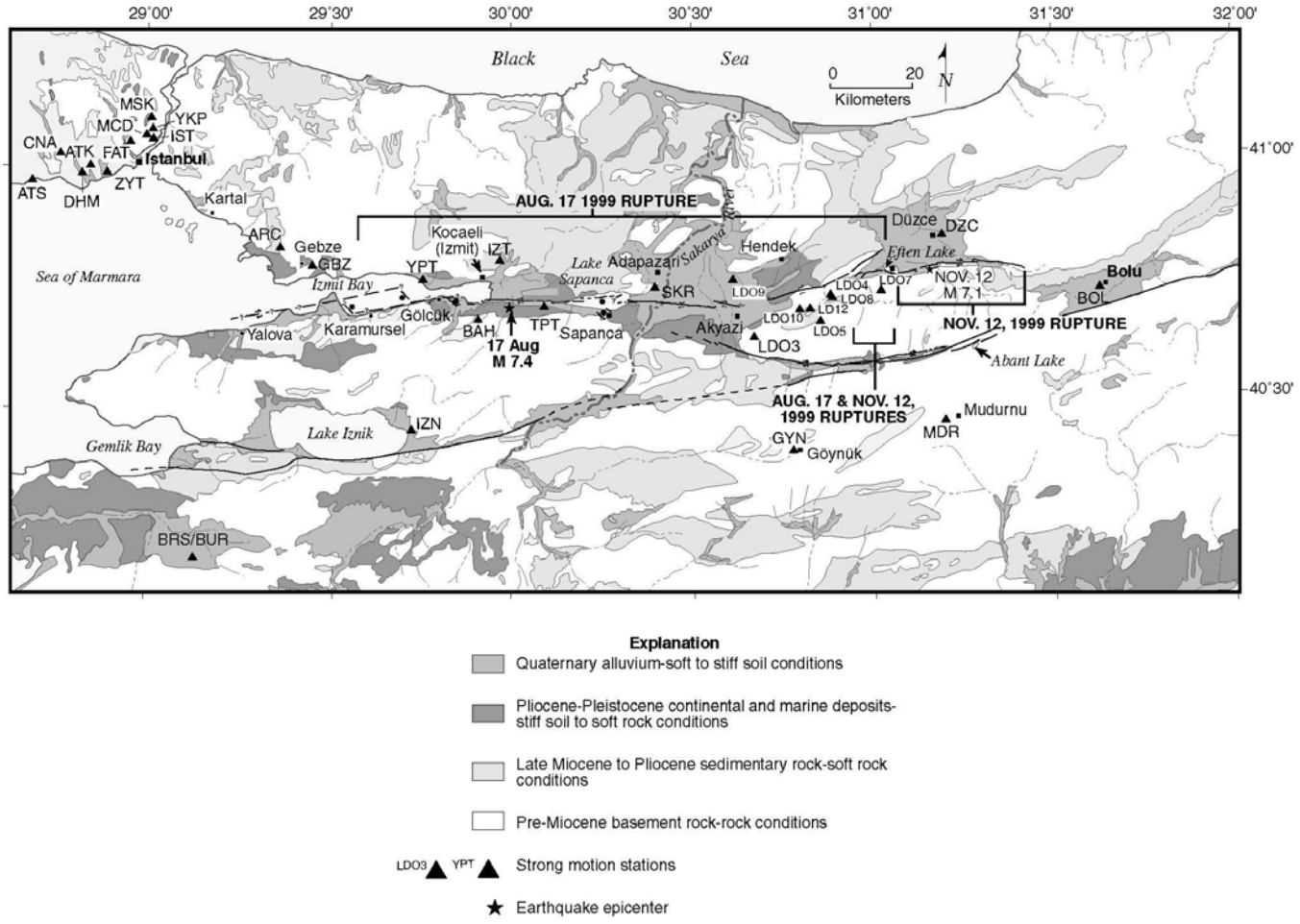

Explanation

- Quaternary alluvium-soft to stiff soil conditions
- Pliocene-Pleistocene continental and marine deposits-stiff soil to soft rock conditions
- Late Miocene to Pliocene sedimentary rock-soft rock conditions
- Pre-Miocene basement rock-rock conditions
- LDO3 ▲ YPT ▲ Strong motion stations
- ★ Earthquake epicenter

Figure 1. Location of Strong Motion Stations
(from William Lettis and Associates)

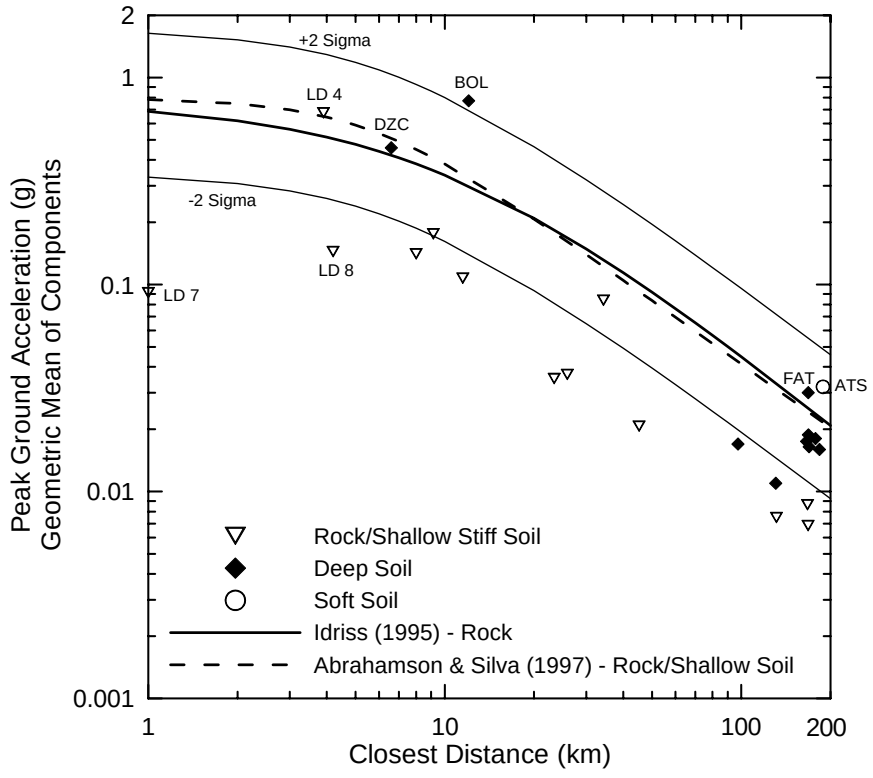

(a)

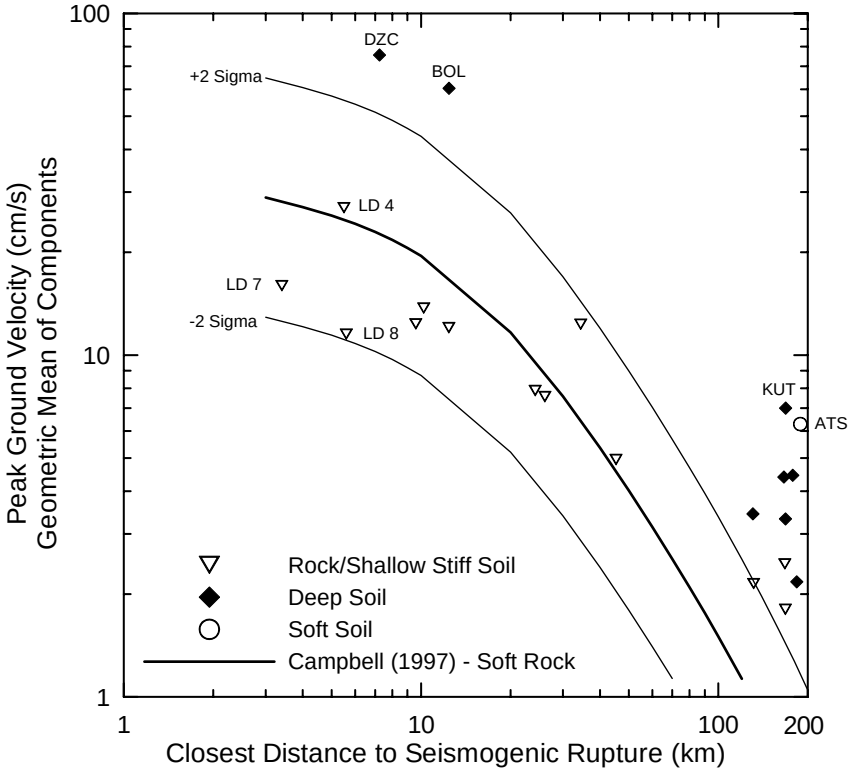

(b)

Figure 2. (a) Recorded peak ground accelerations and ground motion predictive relationships proposed by Idriss (1995) and Abrahamson and Silva (1997), (b) recorded peak ground velocities and ground motion predictive relationship proposed by Campbell (1997).

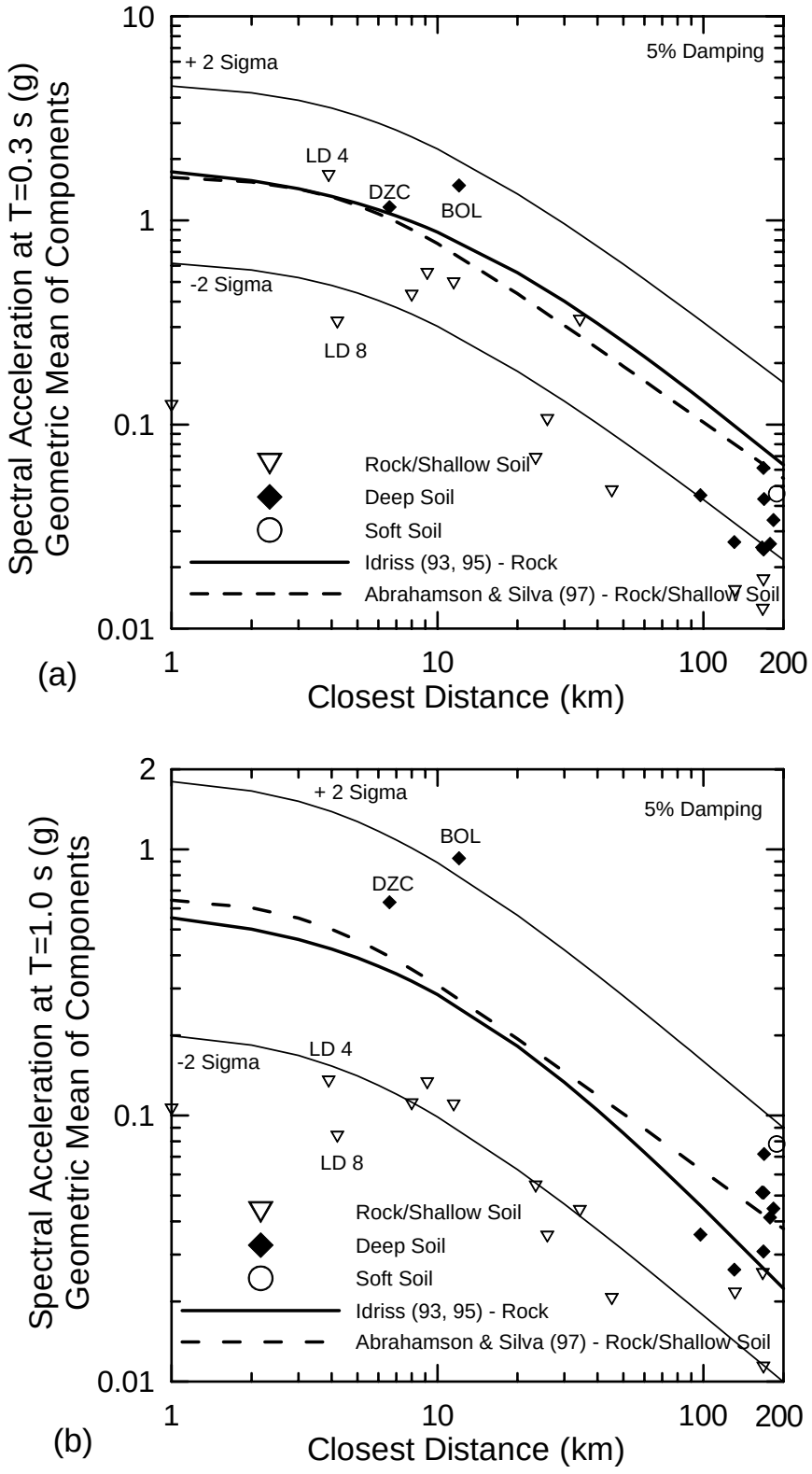

Figure 3. Calculated spectral accelerations at (a) T = 0.3 s and (b) T = 1.0 s and ground motion predictive relationships proposed by Idriss (1993, 1995) and Abrahamson and Silva (1997).

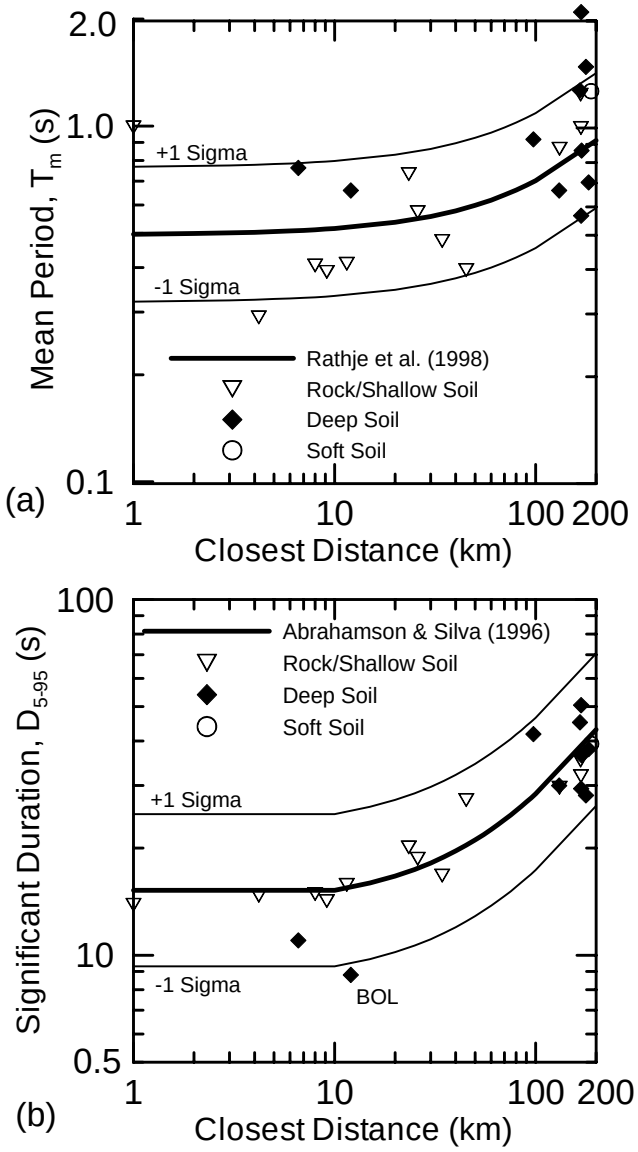

Figure 4. Comparison of (a) mean period and (b) significant duration with predictive relationships proposed by Rathje et al. (1998) and Abrahamson and Silva (1996).

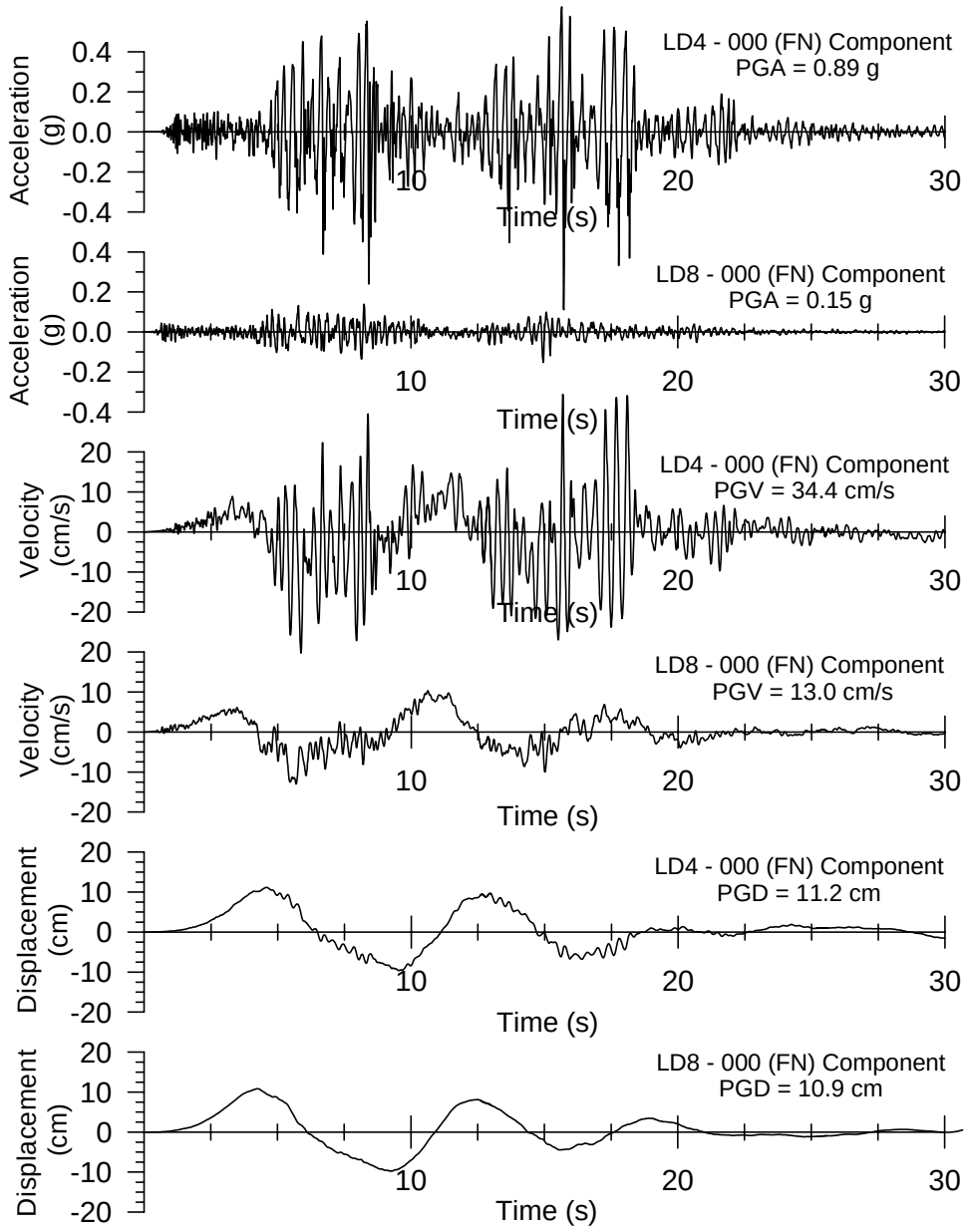

Figure 5. Acceleration, velocity, and displacement-time histories for recordings LD-4 and LD-8.

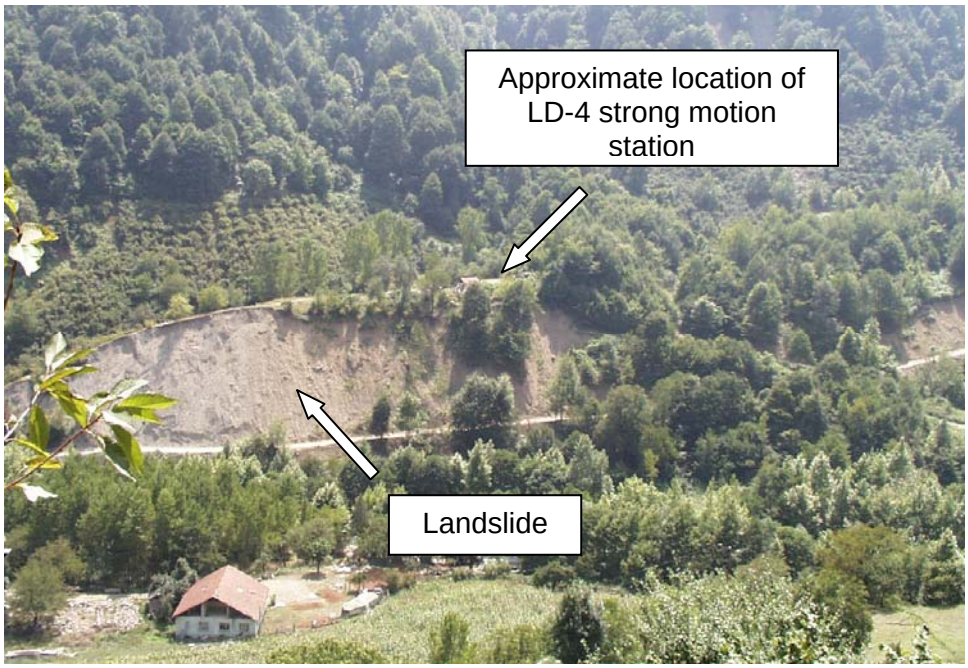

Figure 6. Location of LD-4 strong motion station.

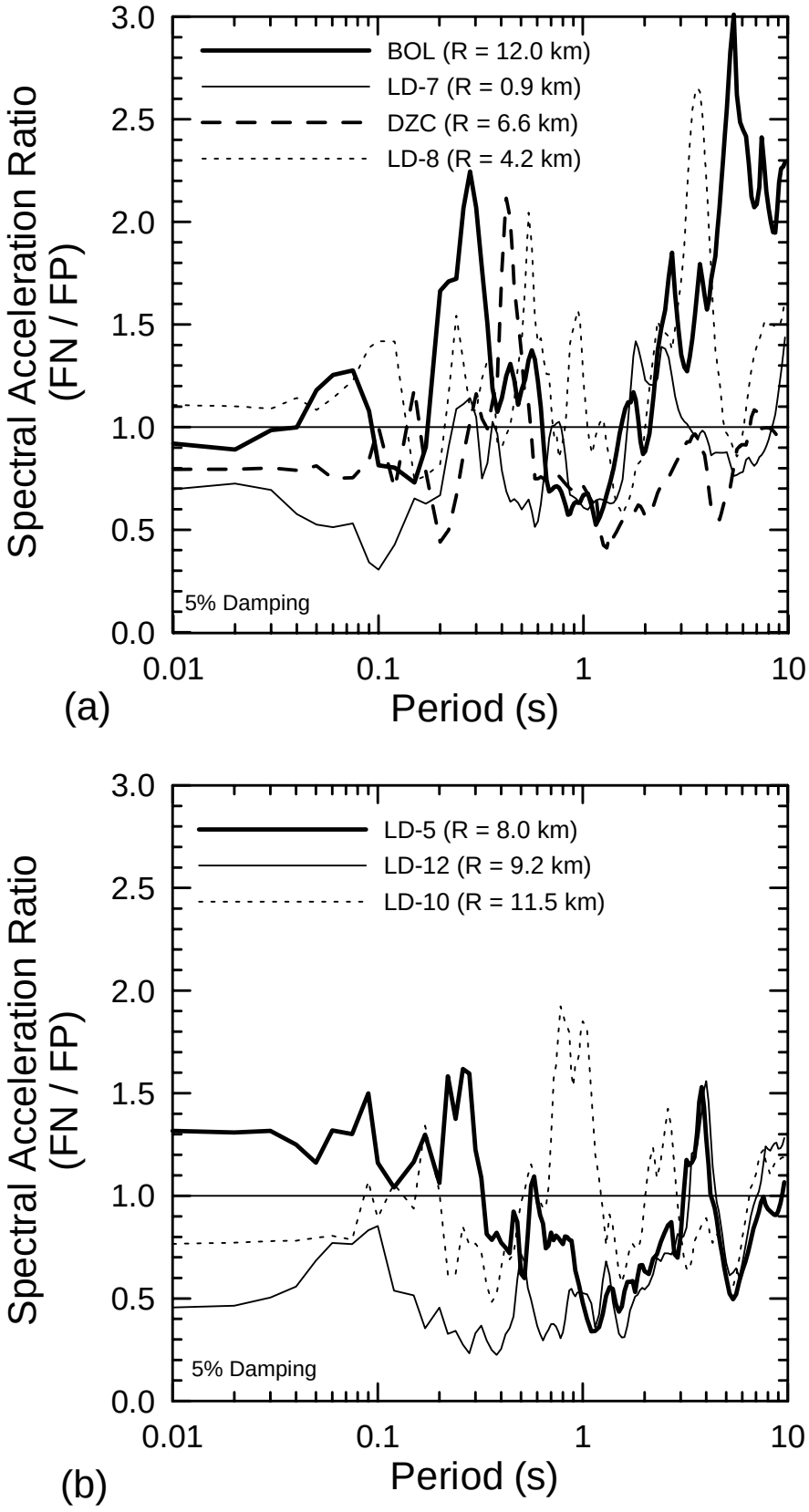

Figure 7. Ratio of fault normal to fault parallel (FN / FP) spectral acceleration for near-fault motions.

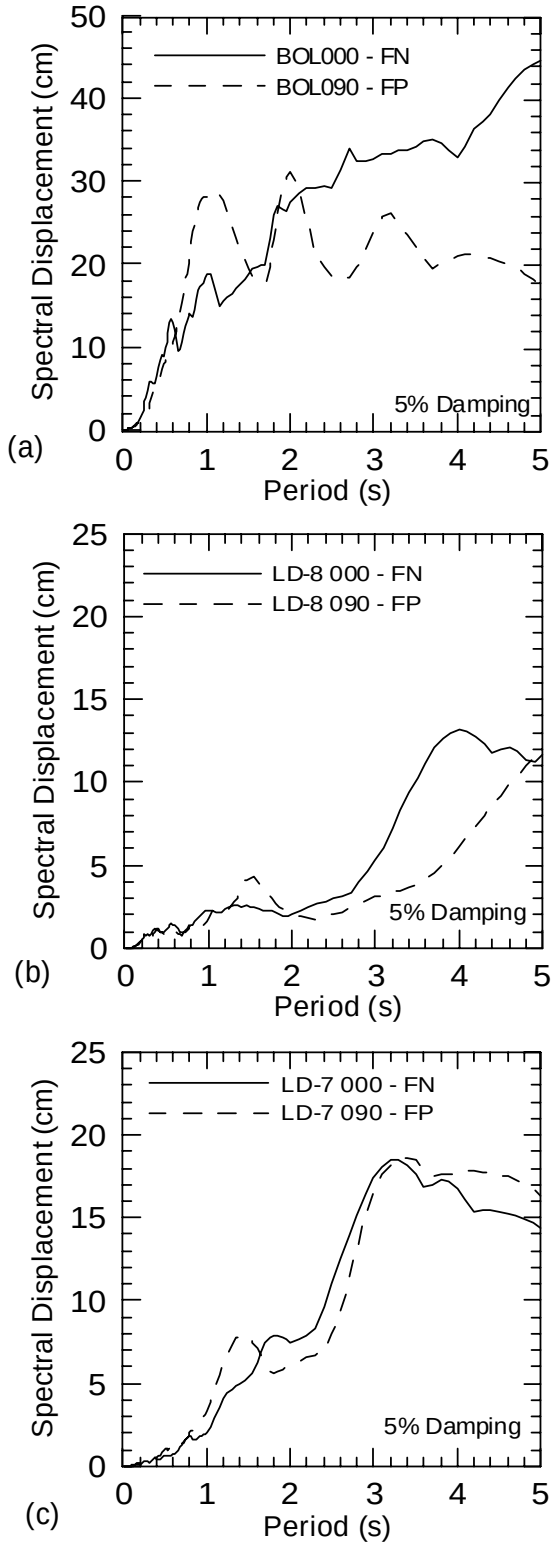

Figure 8. Displacement response spectra for (a) BOL, (b) LD-8, and (c) LD-7 strong motion recordings.

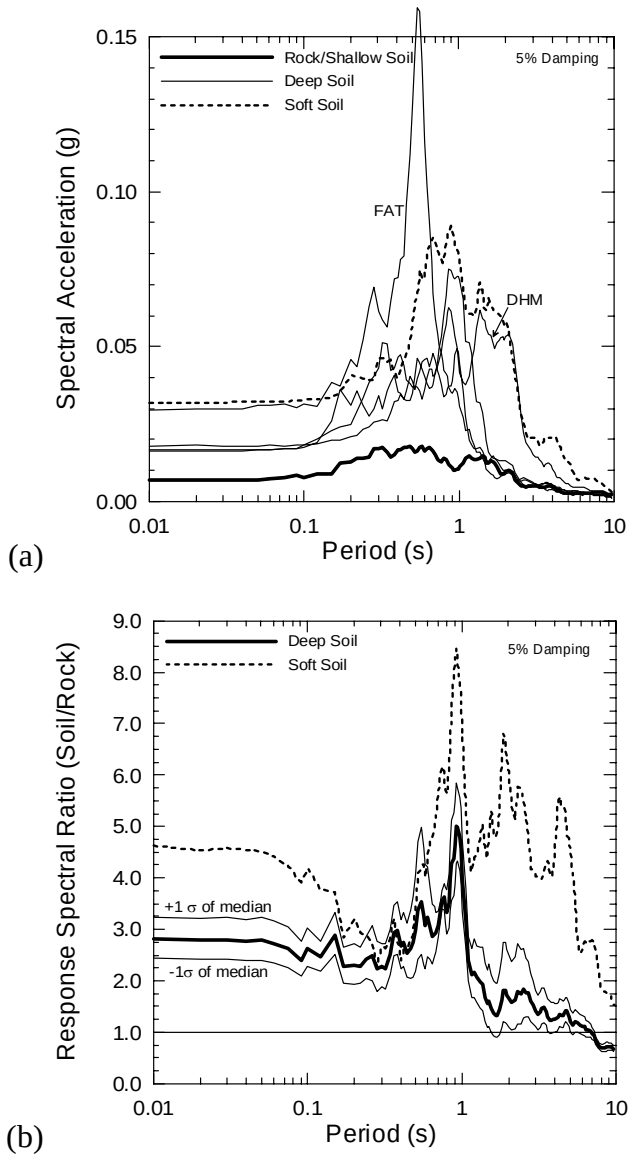

Figure 9. (a) Acceleration response spectra (geometric mean of the two horizontal components), and (b) median response spectral ratios for each site class for motions recorded in Istanbul.

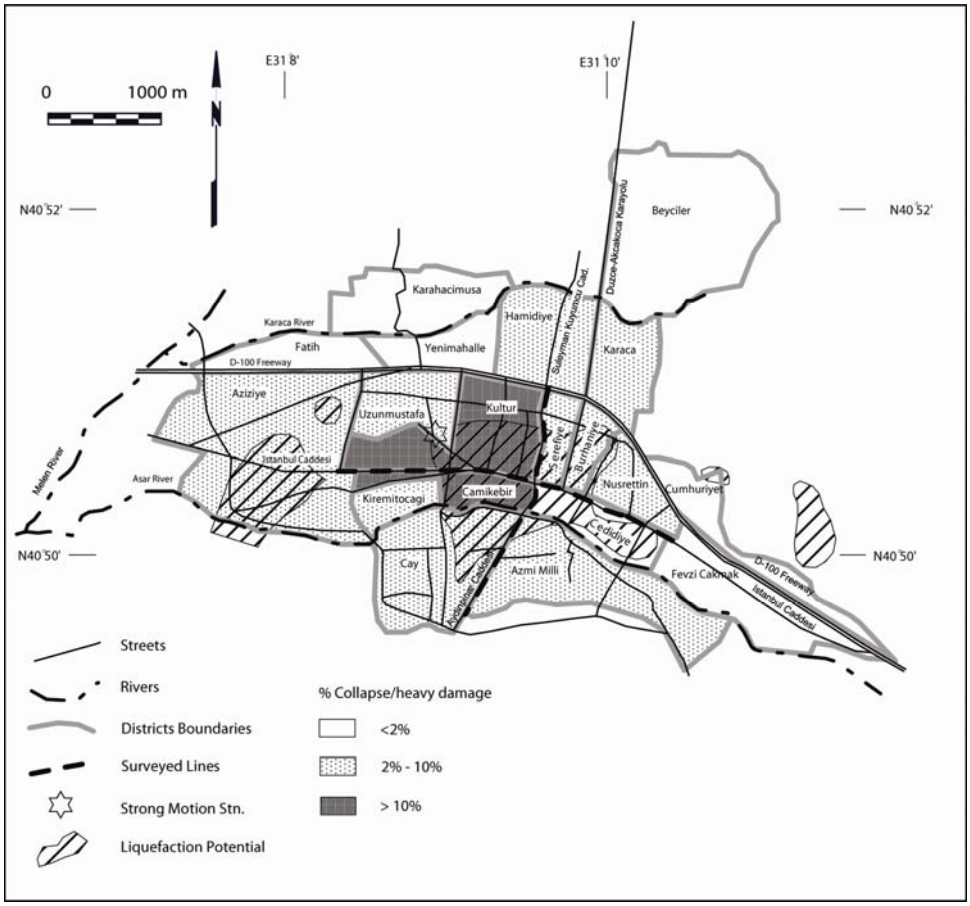

Figure 10. Map of Duzce showing district damage rates and liquefaction susceptible zones by Bayindirlik (2000)

Figure 11. Localized ground settlement of 1 cm adjacent to building (N40.8389, E31.1548)

Figure 12. Collapsed building in Duzce that had already been damaged during the Kocaeli event (N40.83678, E31.1582)

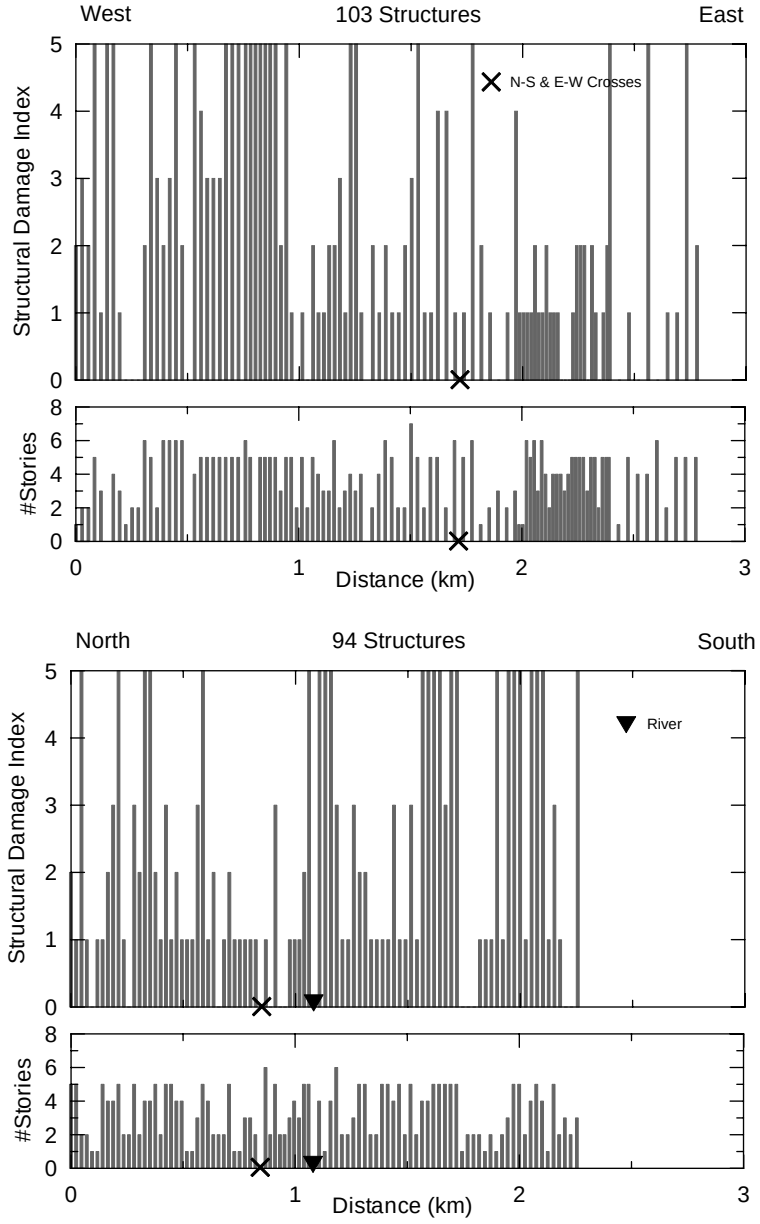

Figure 13. Results of structural damage surveys along East-West and North-South Lines in Duzce: W(N40.5044, E31.0838) to E(N40.50158, E31.1031), N(N40.8454, E31.1603) to S(N40.8276, E31.1526), and Crossing Point at (N40.5035, E31.0958).

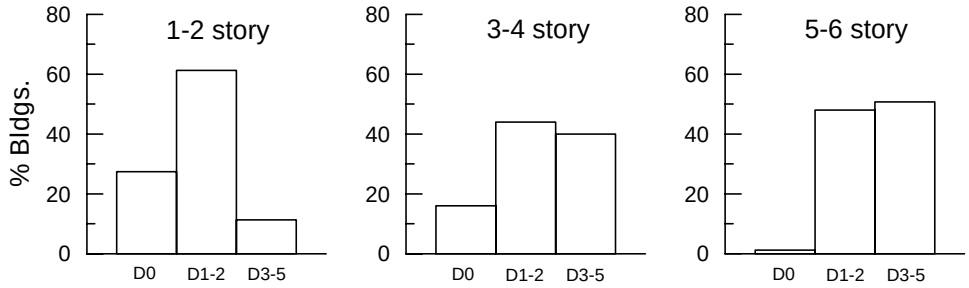

Figure 14. Percentage of damage with respect to number of stories among the 197 surveyed structures in Duzce.


Figure 15. Building in Duzce that had been retrofitted after the 1999 Kocaeli earthquake (N40.5034, E31.0952)

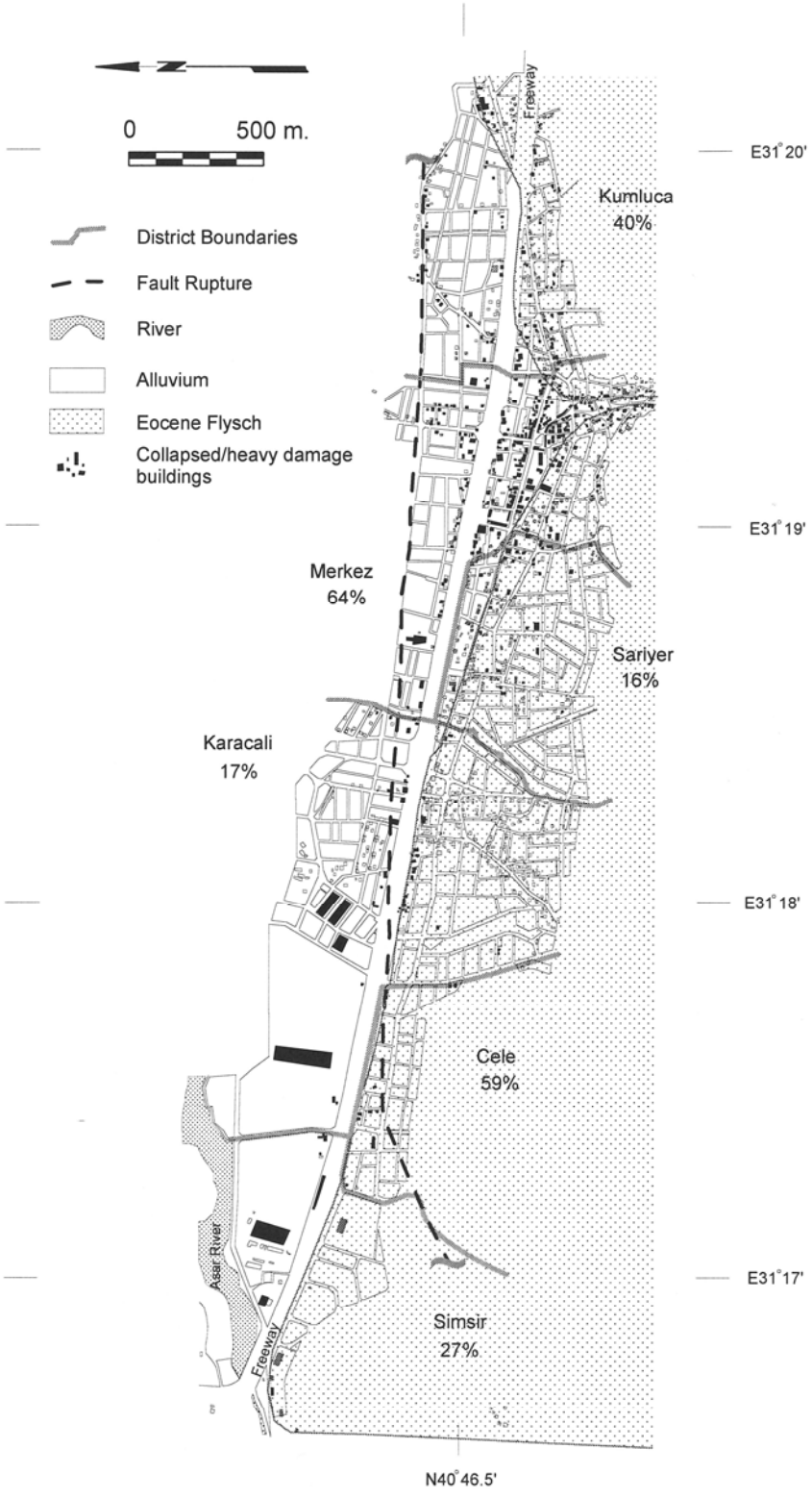

Figure 16. Map of Kaynasli showing surface geology and locations of damaged structures (Kaynasli 2000)

Figure 17. Example of poorly reinforced structure with no bonding between structural members in Kaynasli (N40.4631, E31.1923)

Figure 18(a) View of Merkez District, Kaynasli, looking north
(N40.4629, E31.1931)

Figure 18(b) View of Sariyer district, Kaynasli, looking north-west
(N40.4629, E31.1931)

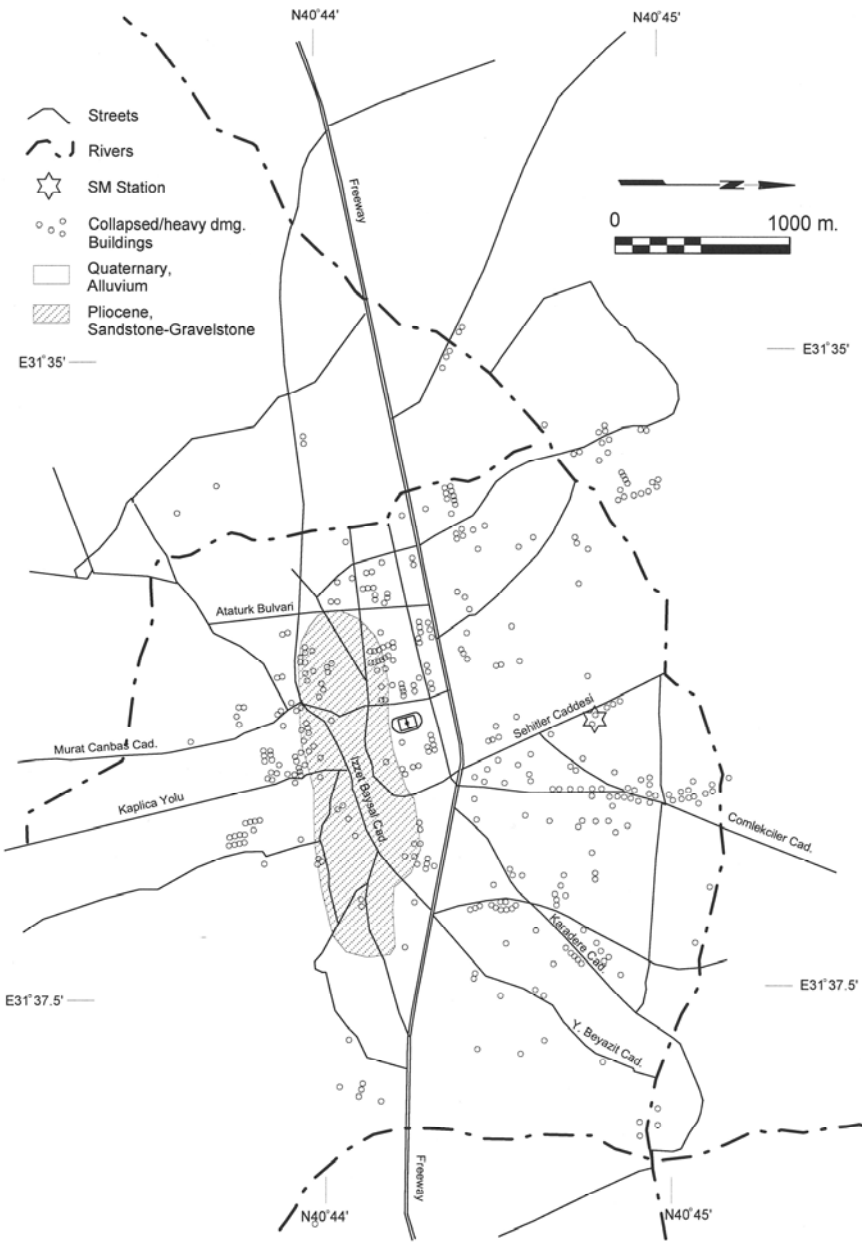

Figure 19. Map of Bolu showing surface geologic conditions and damage patterns (Bolu 2000, Baturay 2000)